



HAL
open science

A gm/ID-Based Noise Optimization for CMOS Folded-Cascode Operational Amplifier

Jack Ou, Pietro Maris Ferreira

► **To cite this version:**

Jack Ou, Pietro Maris Ferreira. A gm/ID-Based Noise Optimization for CMOS Folded-Cascode Operational Amplifier. *IEEE Transactions on Circuits and Systems II: Express Briefs*, 2014, 61 (10), pp.783 - 787. 10.1109/TCSII.2014.2345297 . hal-01074273

HAL Id: hal-01074273

<https://centralesupelec.hal.science/hal-01074273>

Submitted on 13 Oct 2022

HAL is a multi-disciplinary open access archive for the deposit and dissemination of scientific research documents, whether they are published or not. The documents may come from teaching and research institutions in France or abroad, or from public or private research centers.

L'archive ouverte pluridisciplinaire **HAL**, est destinée au dépôt et à la diffusion de documents scientifiques de niveau recherche, publiés ou non, émanant des établissements d'enseignement et de recherche français ou étrangers, des laboratoires publics ou privés.

AUTHOR VERSION

noise parameter. According to this model, γ approaches 1 when the drain-to-source voltage (V_{DS}) approaches zero and decreases to 2/3 when the device enters the saturation regime [2]. A procedure for extracting γ as a function of g_m/I_D , V_{SB} , V_{DS} , and L was described in [4]. If we divide (1) by g_m^2 , we have the thermal noise present at the gate

$$\overline{v_{ng,th}^2} = \frac{4kT\gamma}{g_m}. \quad (2)$$

B. Flicker Noise

Since MOSFETs are surface-conduction devices, flicker noise is important at low frequencies. The flicker noise at the drain terminal is [2]

$$\overline{i_{nd,fn}^2} = \frac{K_f}{C_{ox}WL} \frac{g_m^2}{f} \quad (3)$$

where K_f is a process parameter that depends on the W and L of a transistor [1], C_{ox} is the oxide capacitance, W is the width, and L is the length. At the device noise corner frequency (f_{co}), the thermal noise is equal to the flicker noise

$$\overline{i_{nd,th}^2} = 4kT\gamma g_m = \frac{K_f}{C_{ox}WL} \frac{g_m^2}{f_{co}} = \overline{i_{nd,fn}^2}. \quad (4)$$

We solve (4) to get an expression for f_{co} . Similar to γ , f_{co} is a function of g_m/I_D , as well as V_{SB} , V_{DS} , and L , through its dependence on the current density [4]

$$f_{co} = \frac{K_f}{C_{ox}L} \frac{g_m}{I_D} \frac{I_D}{W} \frac{1}{4kT\gamma}. \quad (5)$$

Multiplying $\overline{i_{nd,fn}^2}$ in (4) by f_{co} , we have

$$\overline{i_{nd,th}^2} f_{co} = \frac{K_f}{C_{ox}WL} g_m^2. \quad (6)$$

Substituting (6) into (3), we have a simple equation that relates the thermal noise current to the flicker noise current

$$\overline{i_{nd,fn}^2} = \overline{i_{nd,th}^2} \frac{f_{co}}{f}. \quad (7)$$

Dividing (7) by g_m^2 , we have the gate-referred flicker noise

$$\overline{v_{ng,fn}^2} = \overline{v_{ng,th}^2} \frac{f_{co}}{f}. \quad (8)$$

C. Gate-Referred Noise Voltage

The total noise at the gate terminal consists of the thermal noise as well as the flicker noise. Using (8) and (2), the total noise at the gate terminal is

$$\overline{v_{ng}^2} = \overline{v_{ng,th}^2} + \overline{v_{ng,fn}^2} = \frac{4kT\gamma}{g_m} \left(1 + \frac{f_{co}}{f} \right). \quad (9)$$

Equation (9) shows that, once I_D is fixed, $\overline{v_{ng}^2}$ (the gate-referred noise) depends on g_m/I_D parameters such as γ and f_{co} .

III. ANALYSIS OF A FOLDED-CASCODE OTA

The noise at the output of the OTA in Fig. 1 is contributed mostly by $M_1 - M_2$, $M_3 - M_4$, and $M_9 - M_{10}$. Assuming that each transistor contributes noise independently, the output-referred noise is

$$\overline{v_{n,out}^2} = 2 \left(A_o^2 \overline{v_{n1}^2} + R_{out}^2 \frac{g_{m5}^2}{(g_{m5} + g_{ds1} + g_{ds3})^2} g_{m3}^2 \overline{v_{n3}^2} + R_{out}^2 \frac{g_{m7}^2}{(g_{m7} + g_{ds9})^2} g_{m9}^2 \overline{v_{n9}^2} \right). \quad (10)$$

We drop “g” from the subscript of the gate-referred noise to simplify the notation. $\overline{v_{n1}^2}$, $\overline{v_{n3}^2}$, and $\overline{v_{n9}^2}$ are the gate-referred noise of M_1 , M_3 , and M_9 as indicated by (9). A_o is the differential gain of the folded cascode, and R_{out} is the output resistance into M_5 and M_7

$$A_o = g_{m1} R_{out} \frac{g_{m5}}{g_{m5} + g_{ds1} + g_{ds3}}. \quad (11)$$

The input-referred noise of the folded-cascode OTA can be obtained by dividing (10) by A_o^2

$$\overline{v_{n,in}^2} = 2 \left(\overline{v_{n1}^2} + \alpha_3^2 \overline{v_{n3}^2} + \alpha_9^2 \overline{v_{n9}^2} \right) \quad (12)$$

where $\alpha_3 = g_{m3}/g_{m1}$ and α_9 is

$$\alpha_9 = \frac{g_{m9}}{g_{m1}} \frac{g_{m5} + g_{ds1} + g_{ds3}}{g_{m5}} \frac{g_{m7}}{g_{m7} + g_{ds9}}. \quad (13)$$

Since M_1 , M_3 , M_5 , M_7 , and M_9 are designed to operate in the saturation region, the self-gain (g_m/g_{ds}) values of these transistors are large, and $\alpha_9 \approx g_{m9}/g_{m1}$.

IV. DESIGN CONSIDERATIONS

A. Design Specifications

We design a low-noise folded-cascode amplifier to demonstrate the tradeoffs using the g_m/I_D design flow. A 130-nm CMOS process with a 1.2-V power supply is used. The specifications are as follows: a slew rate of 7.5 V/ μ s, a load capacitance of 100 pF, a unity bandwidth of 10 MHz, an input/output common mode voltage of 0.6 V, a current consumption of 75 μ A, and a small signal gain in excess of 40 dB. The circuit shown in Fig. 1 required a common-mode feedback (CMFB) circuit (not shown) with a bias current of 37.5 μ A. The maximum device noise corner frequency is 20 kHz. The current ratio (I_{D3}/I_{D1}) is 2.

B. Input Differential Pair

The bias current of M_1 is constrained by the product of the slew rate and the load capacitance. The transconductance of M_1 is constrained by the product of the unity gain bandwidth and the load capacitance. g_{m1}/I_1 is therefore proportional to the ratio of the unity bandwidth and the slew rate [9]. Using the slew rate of 7.5 V/ μ s and the load capacitance of 100 pF, the g_{m1}/I_1 is 16.75 S/A.

The aspect ratio of M_1 is chosen to maximize the gain and minimize the input-referred noise of the OTA while keeping W_1 less than 100 μ m. L_1 was initially set to 4 μ m to maximize g_{m1}/g_{ds1} [see Fig. 2(a)] and minimize $\overline{v_{n1}^2}$ [see Fig. 2(c)].

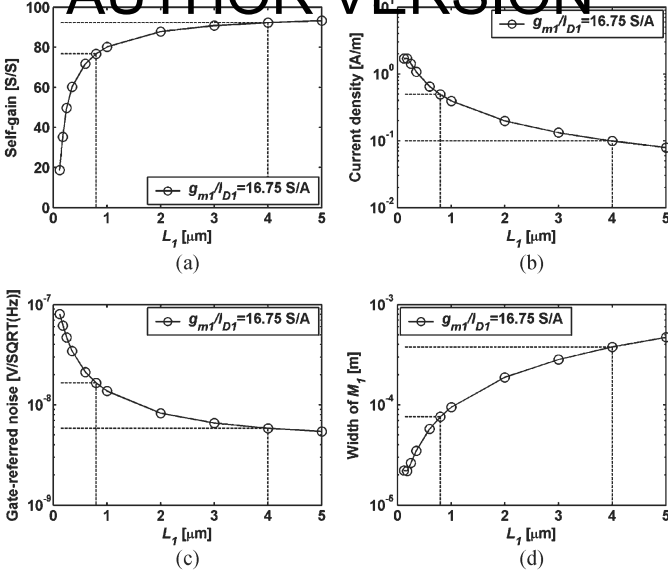


Fig. 2. Tradeoffs of the input differential pair. (a) Self-gain (g_{m1}/g_{ds1}). (b) Current density (I_{D1}/W_1). (c) Gate-referred noise ($\sqrt{v_{n1}^2}$). (d) Width (W_1) of M_1 as a function of L_1 , the length of M_1 . g_m/I_D parameters were extracted and interpolated from transistor-level simulations. $I_{D1} = 37.5 \mu\text{A}$. g_{m1}/I_{D1} is fixed at 16.75 S/A.

Setting L_1 equal to 4 μm , however, increases W_1 beyond 100 μm [see Fig. 2(d)]. To keep W_1 less than 100 μm , the current density of L_1 is increased [see Fig. 2(b)] by reducing L_1 to 0.8 μm at the expense of a slightly lower g_{m1}/g_{ds1} and higher $\sqrt{v_{n1}^2}$. Using $L_1 = 0.8 \mu\text{m}$ and $g_{m1}/I_1 = 16.75 \text{ S/A}$, W_1 is set to 76.20 μm .

C. Cascode Transistor

The aspect ratio of M_5 is designed to maximize g_{m5}/g_{ds5} (and hence A_o) while keeping W_5 less than 100 μm . The gate-referred noise is negligible since M_5 is in a cascode configuration. The design variables are g_{m5}/I_{D5} and L_5 .

The minimum channel length is rarely used in analog design. A reasonable starting point for L_5 , the length of M_5 , is $L_5 = 5L_{\min}$ [10]. The exact starting point for L_5 is not critical. To explore the design space of g_{m5}/I_{D5} and L_5 , the self-gain of M_5 (g_{m5}/g_{ds5}) is plotted in Fig. 3(a) as a function of g_{m5}/I_{D5} at $L = 5L_{\min}$ and $L = 25L_{\min}$. L_{\min} is equal to 120 nm. Fig. 3(a) reveals that g_{m5}/g_{ds5} is maximum for g_{m5}/I_{D5} between 20 and 30 S/A. Therefore, $20 \text{ S/A} \leq g_{m5}/I_{D5} \leq 30 \text{ S/A}$ is used to explore the design space for L_5 .

Fig. 3(c) shows that g_{m5}/g_{ds5} increases with L_5 for $L_5 \leq 0.8 \mu\text{m}$ and saturates for $L_5 > 0.8 \mu\text{m}$. L_5 is set to 0.8 μm to maximize g_{m5}/g_{ds5} without increasing W_5 excessively [see Fig. 3(d)]. g_{m5}/I_{D5} is set to 20 S/A to increase the current density [see Fig. 3(b)] and minimize W_5 without a substantial decrease in g_{m5}/g_{ds5} . The W/L ratio for M_5 is equal to 17.2 $\mu\text{m}/0.8 \mu\text{m}$.

D. Load Transistor

The aspect ratio of M_3 is designed to maximize g_{m3}/g_{ds3} and minimize the gate-referred noise of M_3 . The design variables are g_{m3}/I_{D3} and L_3 .

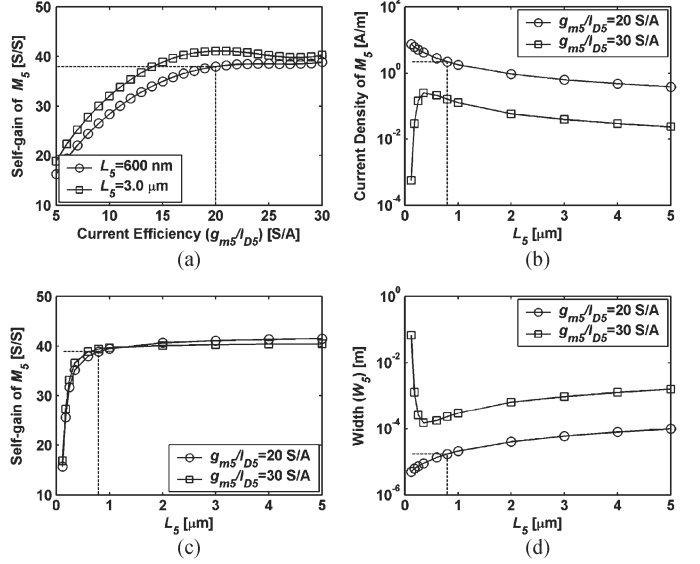


Fig. 3. Tradeoffs of the cascode transistor (M_5). (a) Self-gain of M_5 as a function of g_{m5}/I_{D5} . (b) Current density (I_{D5}/W_{D5}). (c) Self-gain (g_{m5}/g_{ds5}). (d) Width of M_5 as a function of L_5 , the length of M_5 . $I_{D5} = 37.5 \mu\text{A}$. g_m/I_D parameters were extracted and interpolated from transistor-level simulations.

The design space for g_{m3}/I_{D3} is derived as follows. First, according to (5), f_{co} is inversely proportional to L ; therefore, a sufficiently long transistor should be used to minimize f_{co} . Second, as g_m/I_D increases, the current density decreases at a rate faster than the rate at which g_m/I_D increases; therefore, f_{co} decreases with g_m/I_D . (This point is explored further in Section V-B.) Consequently, the minimum g_{m3}/I_{D3} is determined by the f_{co3} requirement. Fig. 4(a) shows that, to keep f_{co3} less than 20 kHz, g_{m3}/I_{D3} must exceed 19 S/A for $L_3 = 3 \mu\text{m}$. A shorter channel length, such as $L_3 = 600 \text{ nm}$, fails to meet the minimum f_{co} requirement for g_{m3}/I_{D3} less than 30 S/A. Third, the maximum g_{m3}/I_{D3} is determined by the minimum g_{m3}/g_{ds3} and the maximum W_3 since both W_3 [see Fig. 4(c)] and g_{m3}/g_{ds3} [see Fig. 4(e)] increase with g_{m3}/I_{D3} . A current efficiency (g_{m3}/I_{D3}) of 25 S/A is chosen as a compromise. For $L = 3 \mu\text{m}$, the design space for g_{m3}/I_{D3} is $19 \text{ S/A} \leq g_{m3}/I_{D3} \leq 25 \text{ S/A}$.

The design space for L_3 is determined as follows. For a $f_{co3} = 20 \text{ kHz}$, the minimum L_3 is 2 μm for $g_{m3}/I_{D3} = 25 \text{ S/A}$ and 3 μm for $g_{m3}/I_{D3} = 19 \text{ S/A}$ according to Fig. 4(b). To keep W_3 less than 300 μm , the maximum L_3 is 2.5 μm for $g_{m3}/I_{D3} = 25 \text{ S/A}$ and 8.0 μm for $g_{m3}/I_{D3} = 19 \text{ S/A}$ according to Fig. 4(d). Fig. 4(f) shows that g_{m3}/g_{ds3} is higher for $g_{m3}/I_{D3} = 25 \text{ S/A}$. We set $g_{m3}/I_{D3} = 25 \text{ S/A}$ to get a higher g_{m3}/g_{ds3} . Based on the discussion so far, we deduce that the design space for L_3 is $L_{3,\min} = 2.0 \mu\text{m} < L < L_{3,\max} = 2.5 \mu\text{m}$. We set L_3 equal to 2.0 μm in order to minimize W_3 . The W/L ratio for M_3 is equal to 248.5 $\mu\text{m}/2.0 \mu\text{m}$.

E. Aspect Ratios of the Remaining PMOS Transistors

The remaining PMOS transistors in Fig. 1 are designed using the same method described in Sections IV-C and IV-D. The aspect ratio for M_7 and M_9 are 89.00 $\mu\text{m}/0.35 \mu\text{m}$ and 48.4 $\mu\text{m}/0.60 \mu\text{m}$, respectively. The g_m/I_D values for M_7 and M_9 are 20 and 15 S/A, respectively.

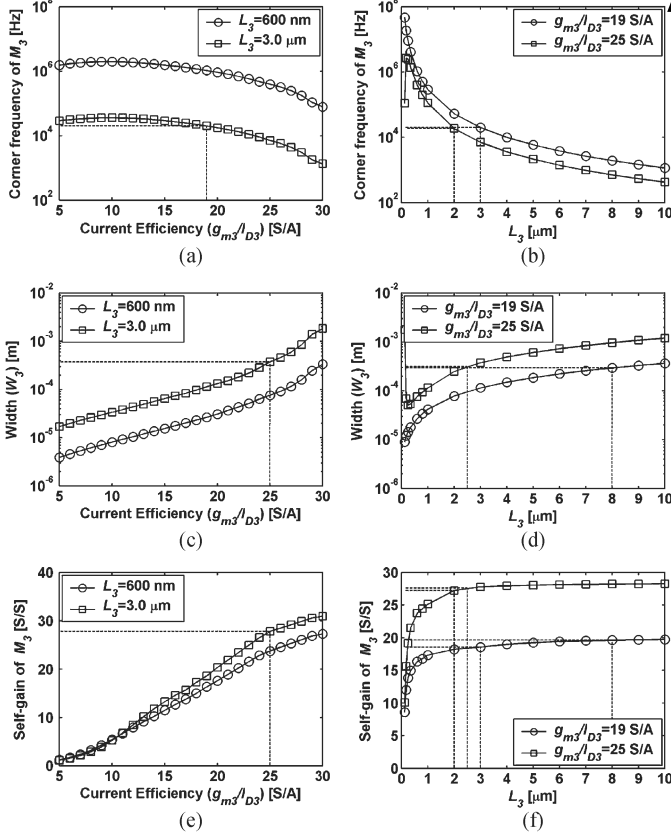


Fig. 4. Tradeoffs of the load transistor (M_3). (a) Corner frequency (f_{co3}), (c) width, and (e) self-gain (g_{m3}/g_{d3}) of M_3 as a function of g_{m3}/I_{D3} of M_3 . (b) Corner frequency, (d) width, and (f) self-gain of M_3 as a function of L_3 , the length of M_3 . $I_3 = 75 \mu\text{A}$. The g_m/I_D parameters were extracted and interpolated from transistor-level simulations.

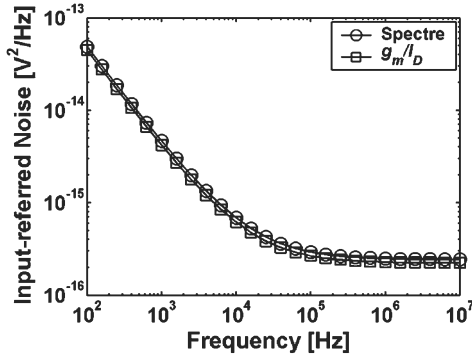


Fig. 5. Comparison of $\overline{v_{n,in}^2}$ simulated using Spectre and $\overline{v_{n,in}^2}$ calculated using the g_m/I_D method.

F. Simulation

Fig. 5 shows the comparison between the input-referred noise of a folded-cascode OTA obtained using Spectre and the input-referred noise calculated with (12). The transistors are modeled using BSIM 4.4. At frequencies lower than the noise corner frequency of the amplifier ($f_{co,ota}$), $\overline{v_{n,in}^2}$ is dominated by the flicker noise of $\overline{v_{n1}^2}$, $\overline{v_{n3}^2}$, and $\overline{v_{n9}^2}$. At frequencies higher than $f_{co,ota}$, $\overline{v_{n,in}^2}$ is dominated by the thermal noise of $\overline{v_{n1}^2}$, $\overline{v_{n3}^2}$, and $\overline{v_{n9}^2}$. Using Spectre as the standard of comparison, the percentage error from 100 Hz to 10 MHz is less than 10.5%.

A. Derivation

In this section, we derive an expression for $f_{co,ota}$ that corresponds to γ and f_{co} of the transistors in the folded-cascode amplifier. We start by rewriting (12) to separate the thermal noise from the flicker noise

$$\overline{v_{n,in,th}^2} = 2 \left(\overline{v_{n1,th}^2} + \alpha_3^2 \overline{v_{n3,th}^2} + \alpha_9^2 \overline{v_{n9,th}^2} \right) \quad (14)$$

$$\overline{v_{n,in,fn}^2} = 2 \left(\overline{v_{n1,fn}^2} + \alpha_3^2 \overline{v_{n3,fn}^2} + \alpha_9^2 \overline{v_{n9,fn}^2} \right). \quad (15)$$

At $f = f_{co,ota}$, $\overline{v_{n,in,th}^2} = \overline{v_{n,in,fn}^2}$. We set (14) equal to (15), replace the gate-referred flicker noise of each transistor using (8), and obtain

$$\overline{v_{n1,th}^2} + \alpha_3^2 \overline{v_{n3,th}^2} + \alpha_9^2 \overline{v_{n9,th}^2} = \overline{v_{n1,th}^2} \frac{f_{co1}}{f_{co,ota}} + \alpha_3^2 \overline{v_{n3,th}^2} \frac{f_{co3}}{f_{co,ota}} + \alpha_9^2 \overline{v_{n9,th}^2} \frac{f_{co9}}{f_{co,ota}}. \quad (16)$$

Solving (16) for $f_{co,ota}$ produces

$$f_{co,ota} = \frac{f_{co1} + \alpha_3^2 \frac{\overline{v_{n3,th}^2}}{\overline{v_{n1,th}^2}} f_{co3} + \alpha_9^2 \frac{\overline{v_{n9,th}^2}}{\overline{v_{n1,th}^2}} f_{co9}}{1 + \alpha_3^2 \frac{\overline{v_{n3,th}^2}}{\overline{v_{n1,th}^2}} + \alpha_9^2 \frac{\overline{v_{n9,th}^2}}{\overline{v_{n1,th}^2}}}. \quad (17)$$

Recall from (2) that $\overline{v_{ng,th}^2} = 4kT\gamma/g_m$. Therefore, $\overline{v_{n3,th}^2}/\overline{v_{n1,th}^2}$ and $\overline{v_{n9,th}^2}/\overline{v_{n1,th}^2}$ in (17) can be simplified to

$$\frac{\overline{v_{n3,th}^2}}{\overline{v_{n1,th}^2}} = \frac{\gamma_3 g_{m1} I_3}{\gamma_1 I_1 g_{m3} I_3} \quad (18)$$

$$\frac{\overline{v_{n9,th}^2}}{\overline{v_{n1,th}^2}} = \frac{\gamma_9 g_{m1} I_9}{\gamma_1 I_1 g_{m9} I_9}. \quad (19)$$

Using (18) and (19), as well as the definition for α_3 and α_9 , $f_{co,ota}$ can be associated with each transistor's f_{co}

$$f_{co,ota} = c_1 f_{co1} + c_3 f_{co3} + c_9 f_{co9} \quad (20)$$

where c_1 , c_3 , and c_9 are defined as

$$c_1 = \frac{1}{1 + \frac{\gamma_3 g_{m3} I_1 I_3}{\gamma_1 I_3 g_{m1} I_1} + \frac{\gamma_9 g_{m9} I_1 I_9}{\gamma_1 I_9 g_{m1} I_1}} \quad (21)$$

$$c_3 = \frac{\frac{\gamma_3 g_{m3} I_1 I_3}{\gamma_1 I_3 g_{m1} I_1}}{1 + \frac{\gamma_3 g_{m3} I_1 I_3}{\gamma_1 I_3 g_{m1} I_1} + \frac{\gamma_9 g_{m9} I_1 I_9}{\gamma_1 I_9 g_{m1} I_1}} \quad (22)$$

$$c_9 = \frac{\frac{\gamma_9 g_{m9} I_1 I_9}{\gamma_1 I_9 g_{m1} I_1}}{1 + \frac{\gamma_3 g_{m3} I_1 I_3}{\gamma_1 I_3 g_{m1} I_1} + \frac{\gamma_9 g_{m9} I_1 I_9}{\gamma_1 I_9 g_{m1} I_1}}. \quad (23)$$

B. Discussion

The ratio of c_3 and c_1 and the ratio of c_9 and c_1 are given by

$$\frac{c_3}{c_1} = \frac{\gamma_3 g_{m3} I_1 I_3}{\gamma_1 I_3 g_{m1} I_1} \quad (24)$$

$$\frac{c_9}{c_1} = \frac{\gamma_9 g_{m9} I_1 I_9}{\gamma_1 I_9 g_{m1} I_1}. \quad (25)$$

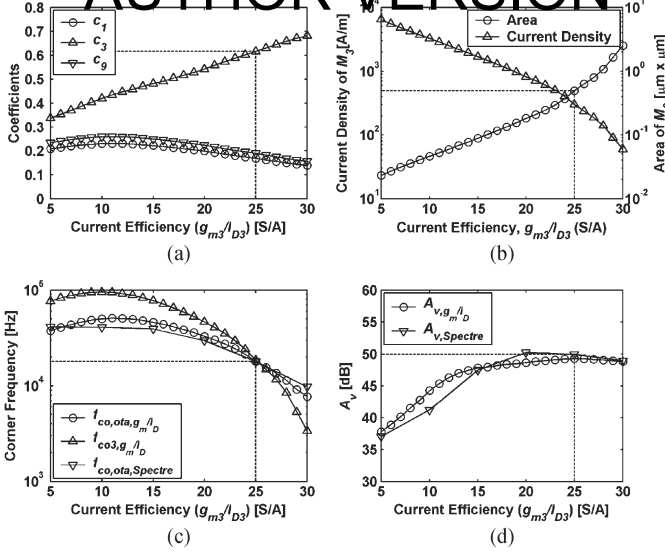


Fig. 6. Tradeoffs of the OTA. (a) Corner frequency coefficients (c_1 , c_3 , and c_9). (b) Area and current density. (c) Contribution of f_{co3} to $f_{co,ota}$. (d) Voltage gain of the OTA as a function of g_{m3}/I_{D3} . $L_3 = 2.0 \mu\text{m}$. $I_3 = 75 \mu\text{A}$.

Using results from Section IV, i.e., $\gamma_3/\gamma_1 = 1.245$, $g_{m3}/I_{D3} = 25$, $g_{m1}/I_{D1} = 16.75$, and $I_3/I_1 = 2$, c_3/c_1 is 3.65. Using γ_9/γ_1 , $g_{m9}/I_{D9} = 15$, and $I_9/I_1 = 1$, c_9/c_1 is 1.125. Since $c_3/c_1 = 3.65$ and $c_9/c_1 = 1.125$, we conclude that $c_3 > c_9 > c_1$.

Since g_{m1}/I_{D1} is determined by the unity gain bandwidth and the slew rate, c_3/c_1 is controlled by g_{m3}/I_{D3} and I_3/I_1 according to (24). We explore the use of g_{m3}/I_{D3} and the current ratio (I_{D3}/I_{D1}) as the design variables next.

The current efficiency of M_3 (g_{m3}/I_{D3}) appears in the denominator of (21) and (23); therefore, both c_1 and c_9 decrease slightly while c_3/c_1 remains constant as g_{m3}/I_{D3} is increased according to Fig. 6(a). According to (24), c_3/c_1 is proportional to g_{m3}/I_{D3} , suggesting that, as g_{m3}/I_{D3} increases, $f_{co,ota}$ becomes increasingly determined by f_{co3} .

The noise corner frequency (f_{co}) of each transistor depends on its g_m/I_D , V_{SB} , V_{DS} , and L . Changing g_{m3}/I_3 , for example, changes f_{co3} , but not f_{co1} and f_{co9} . As g_{m3}/I_{D3} increases, the current density of M_3 is reduced [see Fig. 6(b)] at a rate faster than the increase in g_{m3}/I_{D3} [see (5)]; therefore, f_{co3} is reduced. The decrease in the corner frequency of M_3 as a function of g_{m3}/I_{D3} is shown in Fig. 6(c), as well as the resulting change in the corner frequency of the OTA. As a comparison, we show both the calculated OTA corner frequency ($f_{co,ota,g_m/I_D}$) and simulated OTA corner frequency ($f_{co,ota,Spectre}$) in Fig. 6(c).

The gain of the OTA depends on g_{m3}/g_{ds3} . As g_{m3}/I_{D3} increases, the change in g_{m3}/g_{ds3} observed in Fig. 4(e) results in the saturation of A_V at $g_{m3}/I_{D3} = 20$ in Fig. 6(d). The decrease in current density as g_{m3}/I_{D3} increases results in a corresponding increase in W_3 and, hence, an increase in the

area observed in Fig. 6(b). Fig. 6 confirms our earlier selection of g_{m3}/I_{D3} as the optimum value for noise, gain, and area.

Equation (24) suggests that $f_{co,ota}$ is a function of the current ratio (I_3/I_1). Our calculation shows that $f_{co,ota}$ is, at most, a weak function of the current ratio since I_3/I_1 appears in both the numerator and the denominator of (22). For a $I_3/I_1 = 2$, $f_{co,ota}$ is 17.99 kHz. For a $I_3/I_1 = 1.5$, $f_{co,ota}$ is 17.63 kHz. In other words, a reduction of I_3/I_1 by 25% only leads to a reduction of $f_{co,ota}$ by 2%.

VI. CONCLUSION

Leveraging on the insight gained from our previous work in g_m/I_D -based noise analysis with γ and f_{co} , we use g_m/I_D noise parameters to explore the design space systematically and make transistor-level tradeoff decisions based on requirements for transistor area, noise, and gain. We identify the design bottleneck for the folded-cascode amplifier by developing a closed-form formula for the noise corner frequency of the OTA. The method described in this brief is general and can be applied to design a wide variety of low-noise circuits. Moreover, the noise equations derived in this brief can be integrated in a computer-aided design tool to simplify nanoscale MOSFET circuit design.

ACKNOWLEDGMENT

The authors would like to thank Dr. A. Kujoory and Dr. M. F. Caggiano for their careful review of this brief.

REFERENCES

- [1] P. K. Chan, L. S. Ng, L. Siek, and K. T. Lau, "Designing CMOS folded cascode operational amplifier with flicker noise minimisation," *Microelectron. J.*, vol. 32, no. 1, pp. 69–73, Jan. 2001.
- [2] Y. Tsvividis, *Operation and modeling of the MOS transistor*. New York, NY, USA: McGraw-Hill, 1999.
- [3] F. Silveira, D. Flandre, and P. G. A. Jespers, "A g_m/I_D based methodology for the design of CMOS analog circuits and its application to the synthesis of a silicon-on-insulator micropower OTA," *IEEE J. Solid-State Circuits*, vol. 31, no. 9, pp. 1314–1319, Sep. 1996.
- [4] J. Ou, " g_m/I_D based noise analysis for CMOS analog," in *Proc. IEEE MWCAS*, 2011, pp. 26–29.
- [5] J. Ou, P. Ferreira, and J. C. Lee, "Experimental demonstration of g_m/I_D based noise analysis," *Circuits Syst.*, vol. 5, no. 4, pp. 69–75, Apr. 2014.
- [6] E. Alvarez and A. Abusleme, "Noise power normalisation: Extension of g_m/I_D technique for noise analysis," *Electron. Lett.*, vol. 48, no. 8, pp. 430–432, Apr. 2012.
- [7] E. Alvarez, D. Avila, H. Campillo, A. Dragone, and A. Abusleme, "Noise in charge amplifier—A g_m/I_D approach," *IEEE Trans. Nucl. Sci.*, vol. 59, no. 5, pp. 2457–2462, Oct. 2011.
- [8] J. Ou, " g_m/I_D based distortion analysis," in *Proc. IEEE 10th Int. NEWCAS*, 2012, pp. 61–64.
- [9] D. Stefanovic and M. Kayal, *Structured Analog CMOS Design*. Dordrecht, The Netherlands: Springer-Verlag, 2010, pp. 141–156.
- [10] W. Sansen, *Analog Design Essentials*. Dordrecht, The Netherlands: Springer-Verlag, 2008, p. 47.